Predominant Sea Ice Fracture Zones Around Antarctica and Their Relation to Bathymetric Features

F. Reiser, S. Willmes, Ute Hausmann, G. Heinemann

Geophysical Research Letters

RESEARCH LETTER
10.1029/2019GL084624

Predominant Sea Ice Fracture Zones Around Antarctica and Their Relation to Bathymetric Features

F. Reiser[1], S. Willmes[1], U. Hausmann[2], and G. Heinemann[1]

[1]Environmental Meteorology, University of Trier, Trier, Germany, [2]Sorbonne-Université, LOCEAN-IPSL, Paris, France

Key Points:
- We present the first long-term observed daily Antarctic sea ice leads based on MODIS TIR imagery from 2003-2018
- Sea-ice leads occur along the shelf break and are associated with the Southern Ocean Bathymetry
- Sea ice leads are predominantly found in regions of enhanced tidal divergence

Correspondence to:
F. Reiser,
reiser@uni-trier.de

Citation:
Reiser, F., Willmes, S., Hausmann, U., & Heinemann, G. (2019). Predominant sea-ice fracture zones around Antarctica and their relation to bathymetric features. *Geophysical Research Letters*, *46*, 12,117–12,124. https://doi.org/10.1029/2019GL084624

Received 19 JUL 2019
Accepted 25 SEP 2019
Accepted article online 17 OCT 2019
Published online 13 NOV 2019

Abstract Sea ice is of substantial importance for the Southern Ocean, as it insulates the relatively warm ocean from the cold atmosphere. Due to mechanical stress induced by wind and ocean currents, sea ice leads occur, which are characterized by open water and thin ice causing an increase of energy and moisture fluxes between ocean and atmosphere. Furthermore, they contribute to the ice production and provide a habitat for animals. Thus, it is important to gain information about the temporal and spatial distribution of leads on a circum-Antarctic scale. So far, no operational data set exists, which provides such information. We use thermal satellite imagery from the Moderate Resolution Imaging Spectroradiometer to derive the predominant lead patterns for 2003–2018, April–September. This study provides first results for the long-term average lead frequencies in the Southern Ocean and discusses possible links to ocean currents, tides, and the bathymetry.

Plain Language Summary The polar regions are strongly influenced by sea ice, which covers large areas of the ocean's surface. Interacting with the atmosphere and the ocean, sea ice is a very dynamic surface with a large temporal and spatial variability. Under the forcing of winds and ocean currents, sea ice is subject to deformation processes causing cracks (leads) in the ice. The observation of these leads is the aim of this study since they are an important feature. For instance, open water can be found in these cracks, which enables the warm ocean (−1.7 ° C) to lose energy to the cold atmosphere. Also, sea ice forms a habitat for animals. In this study, the focus is on the Southern Hemisphere where sea ice surrounds the Antarctic continent. For the winter months, we use thermal infrared satellite images where leads appear as warm, almost linear features compared to the cold ice cover. By using computer algorithms, the cracks are detected automatically. This is the first study that shows these features in the Southern Ocean. Leads not only exist close to the coastline but also tend to appear offshore with characteristic spatial patterns. Therefore, possible links to ocean currents, tides, and bathymetry are discussed.

1. Introduction

Sea ice is crucial in its relevance for the climate system both on regional and global scales and has a large seasonal and interannual variability (Turner et al., 2015). Since sea ice acts as an insulator, it modulates the exchange processes between the relatively warm ocean and the atmospheric boundary layer. Cracks in the pack ice in which open water or thin ice are present are therefore major sources for heat and moisture release to the atmosphere (Alam & Curry, 1995; Maykut, 1978; Smith et al., 1990), as well as for sea ice production and dense water formation (Ohshima et al., 2013; Zwally et al., 1985). Although leads cover only a small proportion of the sea ice surface, their contribution to the total heat exchange of the pack ice region is enormous (Chechin et al., 2019; Lüpkes et al., 2008; Marcq & Weiss, 2012). Furthermore, they also provide a habitat for mammals and seabirds (Stirling, 1997). Besides polynyas, which are larger and spatially persistent openings (Smith et al., 1990), leads occur more randomly within the pack ice due to divergence induced by wind and ocean stress.

The detection and investigation of sea ice leads in the Arctic Ocean have been put forward by several studies using either thermal infrared satellite images (Willmes & Heinemann, 2015, 2016) or microwave data (Murashkin et al., 2018; Röhrs & Kaleschke, 2012). In the Southern Ocean, however, long-term and large-scale investigations have mainly focused on the dynamics and variability of polynyas (Kern, 2009; Paul et al., 2015; Tamura et al., 2008; Zwally et al., 1985) and the location and extent of fast ice areas (Fraser et al., 2012), while accurate observations of lead locations and predominant spatial patterns are not available so far. Passive microwave sea ice concentrations (Spreen et al., 2008) are too coarse to resolve narrow leads in

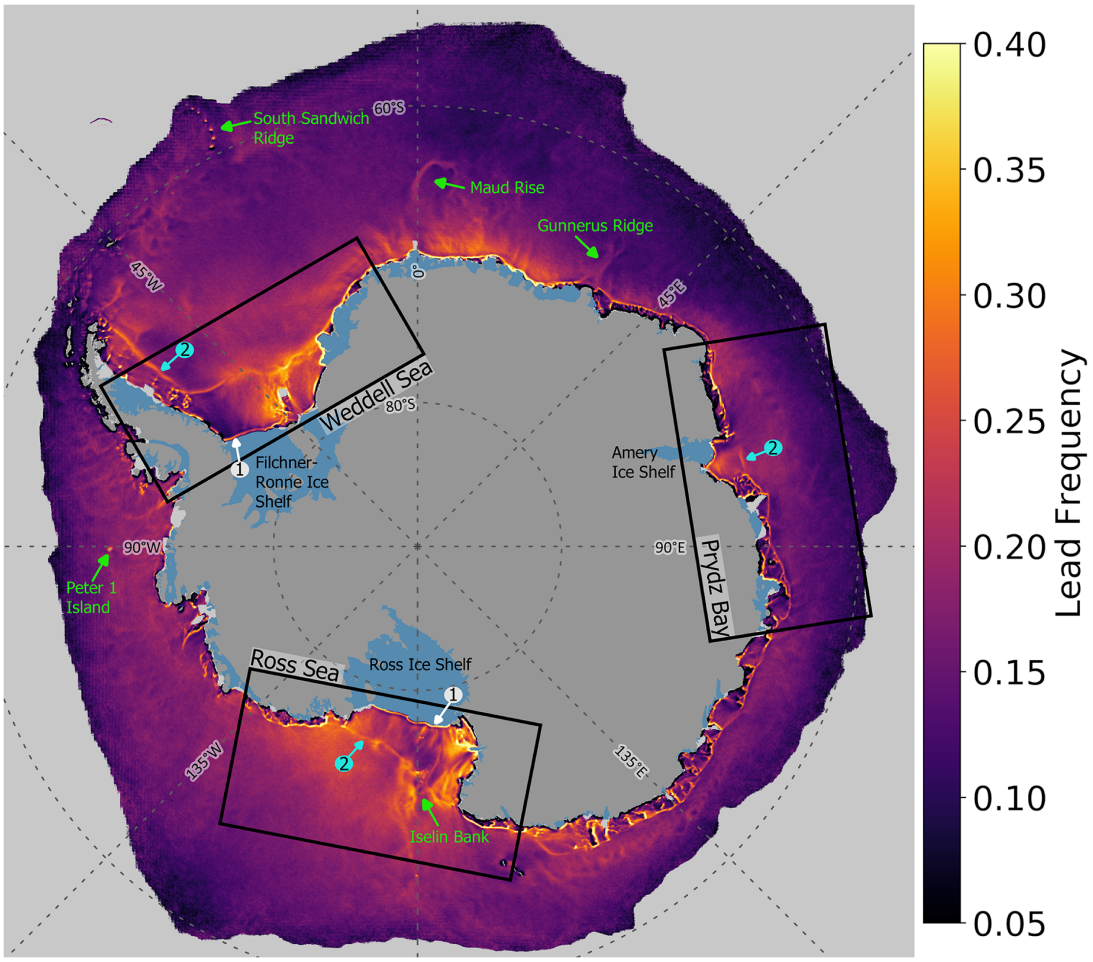

Figure 1. Observed lead frequencies based on daily composites from 2003 to 2018 for winter months only (April to September). Data are retrieved with the lead detection algorithm introduced by Willmes and Heinemann (2015) based on Moderate Resolution Imaging Spectroradiometer thermal infrared satellite data. The area shown corresponds to the maximum sea ice extent observed between 2003 and 2018. The black boxes indicate the location of the three areas of interest presented in Figure 2. The colored arrows indicate interesting locations, for example, increased lead frequencies along the shelf break.

the pack ice, and numerical models cannot simulate leads explicitly. Data sets with daily high-resolution sea ice structures on the kilometer scale are needed as boundary conditions and for the verification of sea ice representation in convective-scale weather prediction models and sea ice ocean models (Müller et al., 2017; Wang et al., 2016). Therefore, similarly to the work of Willmes and Heinemann (2015) for the Arctic, this study presents results based on the long-term lead retrieval from the Moderate Resolution Imaging Spectroradiometer (MODIS) thermal satellite imagery.

Furthermore, the results are discussed in context with oceanographic features, which is suggested by multiple modeling studies, for example, Tamsitt et al. (2017), Hellmer et al. (2012), Kerr et al. (2018), Schmidtko et al. (2014), Robertson (2005), and Koentopp (2005). In Tamsitt et al. (2017) upwelling along the continental shelf break is shown by using the southern ocean state estimate model, which is associated with the Antarctic Coastal Current. The interaction of this current with sea ice is investigated in Hellmer et al. (2012) with the Bremerhaven Regional Ice-Ocean Simulations model.

The influence of tides is also regarded as a major source for mechanical stress on the sea ice cover (Koentopp, 2005; Padman et al., 2002). Koentopp (2005) found that the sea ice concentration and thickness is decreased when tidal forcing is included in the model, in particular over the continental shelf. This is supported by a model for the Weddell Sea, Prydz Bay, and Ross Sea, which shows that the impact of tides is largest over the continental shelf and shelf break (Padman et al., 2002).

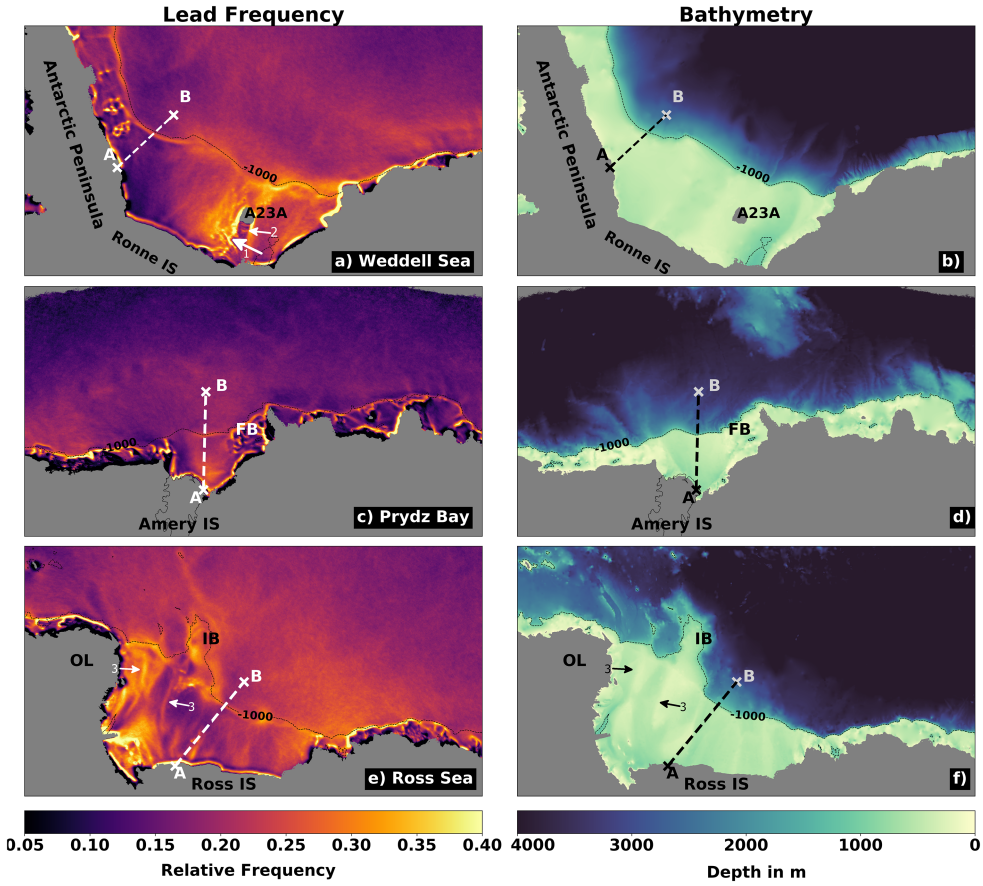

Figure 2. Detailed view of the Weddell Sea (upper row), Prydz Bay (middle row), and Ross Sea (bottom row). The left column shows the relative lead frequency (same as in Figure 1); the right column shows the bathymetry (Schaffer & Timmermann, 2016). The 1,000 m isobath is added to all images for reference. The iceberg A23A (A23A) in the Weddell Sea, the Four-Ladies Bank (FB) in the Prydz Bay, and the Iselin Bank (IB) and Oats Land (OL) are also shown as reference in the maps. The white arrows in (a) and (e) indicate further interesting features.

Recently, Stewart et al. (2019) conducted a comprehensive model study of the Southern Ocean revealing the effects of winds, tides, and eddies on the Antarctic Slope Current. They show that along the shelf break, the mean surface zonal velocity of the ocean is increased, which in turn accelerates the sea ice drift.

These model studies are supported by several observational studies that rely on drifting buoy data and satellite imagery. Ice drift data from buoys deployed 2004 in the western Weddell Sea suggest the presence of a shear zone, which follows the boundary current along the shelf break (Heil et al., 2008; Hutchings et al., 2012). Therefore, small openings in the pack ice are favored; however, the ice concentration derived from AMSR-E passive microwave data remains above 90%, suggesting a closed pack ice area. Furthermore, they found that the correlation between the ice drift and wind velocity was moderate during the investigation period. Instead, it is expected that local bathymetry mainly influences the deformation of the pack ice. Mack et al. (2013) found that tides explain most of the variance in the wintertime sea ice concentration for a study area in the Ross Sea, and they further state that this causes a divergence of sea ice cover, which in turn forms areas of open water and subsequently leads. The mentioned studies show detailed observation data, though they are spatially and temporally limited. Furthermore, AMSR-E satellite passive microwave data are used to obtain sea ice concentration data. Due to the coarse resolution, it was not possible to detect leads explicitly.

In this study, observations of the dominant lead patterns in the Southern Ocean for the past 16 years are presented on a circum-Antarctic scale. Possible links to the bathymetry and ocean circulations are discussed, and a review of published results from different model simulations and field data is provided. In section 2, data and methods are presented. In section 3, the results are described, followed by an overall discussion in section 4. In section 5 the results are summarized, and conclusions are drawn.

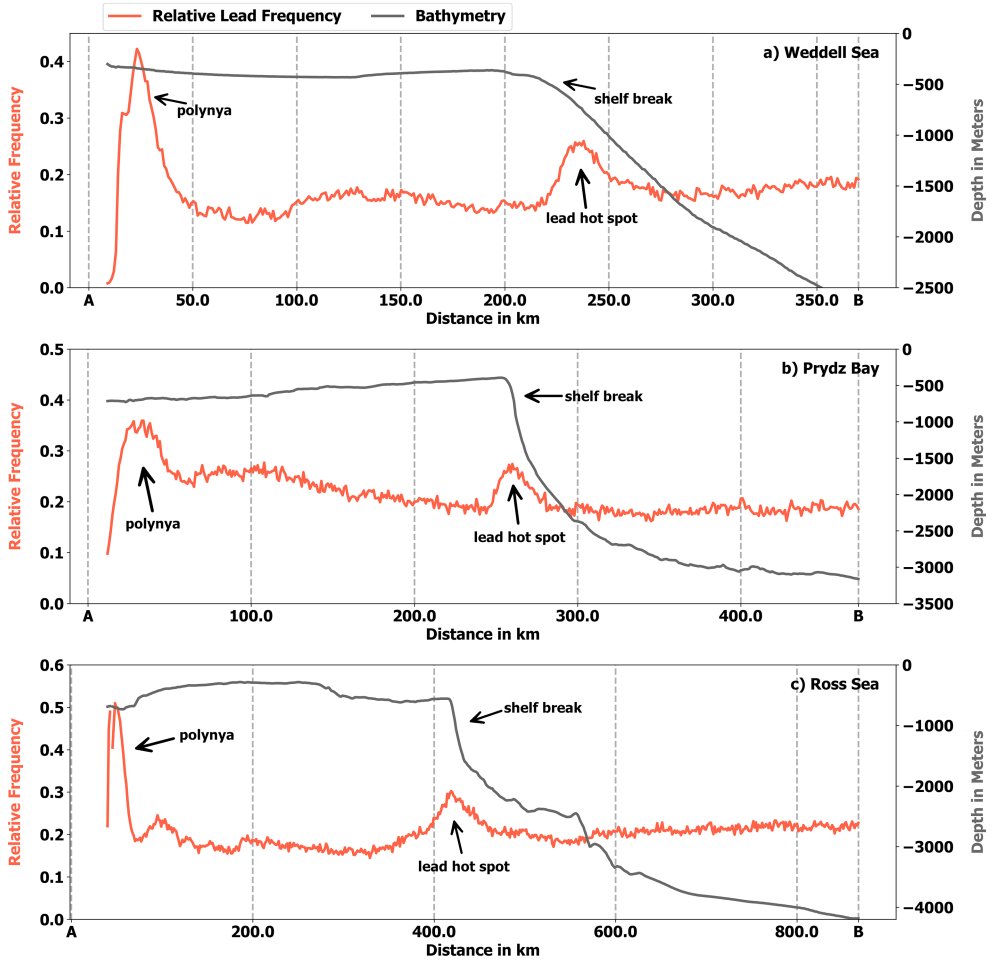

Figure 3. Extracted lead frequency (red) and bathymetry (gray) along the transects for Weddell Sea (a), Prydz Bay (b), and Ross Sea (c). The position of the transects is shown in Figure 2.

2. Data and Methods

Daily circum-Antarctic lead frequencies are retrieved from the MODIS Ice Surface Temperature (MOD29/MYD29) data provided by the National Snow and Ice Data Center (Riggs & Hall, 2015). The product is used as Collection 6, Level 2 swath data and has a spatial resolution of 1 km at nadir. Sea ice concentration from passive-microwave data using the ARTIST Sea Ice (ASI) algorithm (Spreen et al., 2008) is used to mask out non-sea ice areas to reduce the computational effort. The lead-retrieval algorithm introduced by Willmes and Heinemann (2015) was adapted for the Southern Hemisphere. We use all suitable MOD29/ MYD29 granules covering the area south of 50°, which corresponds to more than 500,000 single files for the time period 2003 to 2018, April to September. Only clear-sky pixels are taken into account. Leads are identified as positive local surface temperature anomalies in each MODIS data tile. All tiles are subsequently combined to daily composites, where the average daily lead occurrence is calculated pixel wise from all observations per day.

In order to support our observations, we examine the ocean processes for the Weddell Sea using outputs from a regional model configuration developed using the coupled ocean-sea ice model NEMO-LIM 3.6 (Madec, 2008). The model is used to describe the surface ocean currents and the impact of tides by showing the divergence in the upper ocean layer including tidal forcing. Here, a 5-year average climatology is retrieved for April through September and compared to our sea ice lead frequencies. Based on these data, a case study for the Weddell Sea is conducted, and we anticipate results to be of relevance for other circum-Antarctic regions.

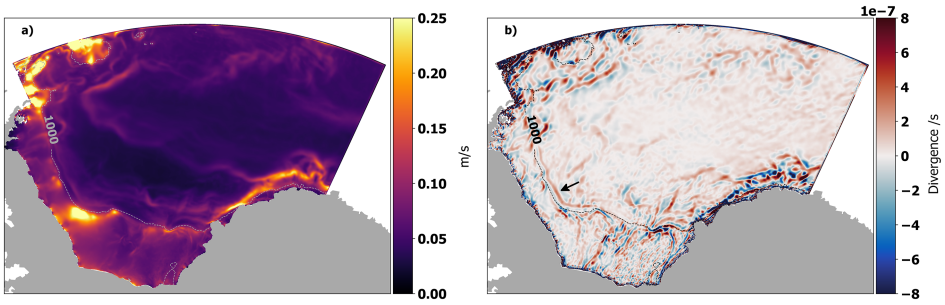

Figure 4. Winter time-average surface speed from a regional model configuration developed using the coupled ocean-sea ice model NEMO-LIM 3.6 (Madec, 2008) including tides (a), and in (b) the surface divergence as extracted from (a).

Being aware that different types of models and specific configurations have been used to examine surface currents and tides in the Southern Ocean, we will address the findings of other model studies in section 4 to assure a comprehensive perspective on this topic.

In the following, we present and discuss the predominant patterns of circum-Antarctic sea ice lead occurrences. Results are analyzed with a focus on three main regions, namely, Weddell Sea, Prydz Bay, and Ross Sea and in context with possible influences from bathymetry (Schaffer & Timmermann, 2016), ocean currents, and tides.

3. Results

The observed long-term average sea ice lead frequencies in the Southern Ocean reveal distinct regions of increased lead activities, which are spatially very strongly bounded (Figure 1). Polynyas north of the Filchner/Ronne and Ross Ice shelves are characterized by the highest lead frequencies (white Arrows 1 in Figure 1), but more surprisingly, there are many more hot spots, where leads apparently open up more regularly than in other regions. Multiple linear patterns of increased lead frequencies are present. A distinct line can be seen close to the coastline almost around the entire continent, but north of the well-known polynyas (cyan Arrows 2 in Figure 1). In the Weddell Sea, Prydz Bay, and Ross Sea further lead hot spots are present along the shelf break and along ridges in the deep sea, for example, Maud Rise or Gunnerus Ridge (see green marker in Figure 1). In the vicinity of islands, for example, along the South Sandwich Ridge or Peter 1 Island (green arrows), sea ice tends to break up more often forming local hot spots. But also in other sectors of the Antarctic Ocean, sea ice leads appear to follow a characteristic, nonrandom spatial pattern. In Figure 2 the subsets indicated in Figure 1 are presented in detail together with the bathymetry for the respective region. The shelf break is indicated by the 1,000-m isobath (dashed line) in all maps. The bathymetry data for the Weddell Sea clearly show the continental shelf area with depths around 400–500 m (Figure 2b). A comparison with Figure 2a indicates that increased lead frequencies can be observed along the shelf break with values exceeding 0.3. North of this narrow band the sea floor topography drops to depths of more than 4,000 m. Further "bright" features (high lead frequencies) can be seen close to the coastline and around the iceberg A23A in the southeastern Weddell Sea (Figure 2a). In the Prydz Bay region, increased lead frequencies are clearly visible near the coast (Figure 2c). Furthermore, a distinct but less pronounced line of increased lead frequencies as in Figure 2a is visibly following the shelf break. Also in the Ross Sea, the lead frequency is increased close to the coastline and along the shelf break (Figure 2e). Around Iselin Bank (IB), lead frequencies are substantially increased, indicating a local hot spot for lead formation. The seabed above the shelf is 400–500 m deep and drops then to more than 4,000-m depth. The IB thereby reaches far into the deep sea with moderate depths, which corresponds to the increased lead frequencies. Remarkably, there are significant lead patterns also on the shelf, which are apparently connected with smaller channels and ridges. This is especially evident in the Weddell Sea around A23A (Figure 2a white arrows), where the fast ice edge (Arrow 1) and the movement of the iceberg (Arrow 2) is visible, and over the eastern Ross Sea Shelf (Figure 2e white arrow), where ridges and troughs in the ocean bathymetry (Arrow 3) can be inferred.

All extracted data along to Transects A and B shown in Figure 2 are presented in Figure 3, for the Weddell Sea (WS), Prydz Bay (PB), and Ross Sea (RS), to illustrate the lead frequency gradients along the ocean bathymetry. All three transects indicate that the position of the shelf break and local lead frequency maxima

overlap in their position. In the Weddell Sea transect (Figure 3a) the seabed stays almost at a constant depth and starts then to descend rapidly after 200 km. Accordingly, the lead frequency increases in the area of the shelf break up to 0.28. The transect in the Prydz Bay (Figure 3b) shows that the sea floor ascends slightly to the shelf break at around 260 km. The pronounced drop in depth is associated with an enhanced lead activity. In the Ross Sea similar results can be found (Figure 3c).

Figure 4 shows the ocean surface speed from the NEMO-LIM 3.6 model including tidal forcing (Figure 4a) and the corresponding divergence (Figure 4b). The simulation shows the band of increased surface speeds following the continental slope, namely, the Antarctic Slope Current. Additionally, the results in Figure 4b show positive divergence along the eastern side of the Antarctic Peninsula (black arrow).

4. Discussion

Our data show that sea ice leads are present throughout the Southern Ocean with predominant features along the coastline, the shelf break, and several ridges (Figure 1). Close to the coastline lead frequencies are increased since also coastal polynyas are detected due to their positive surface temperature anomaly. The polynyas are mainly driven dynamically by wind systems, for example, cold winds from the ice shelf or ice sheet (Paul et al., 2015), causing high energy fluxes compared to the surrounding pack ice (Maykut, 1982), and the formation of new ice and the production of cold and dense water (Haid et al., 2015; Tamura et al., 2008). The stability of sea ice depends highly on the stresses acting on it. Both wind and ocean currents can cause divergence or convergence of the ice drift, hence leading to thinner ice or ice breakup, or to thicker and partially rafted ice, respectively. Holland and Kwok (2012) found the vector correlation between the sea ice drift and 10-m wind to be low above the shelf in the Weddell Sea and in the western parts of the Ross Sea. Thus, it can be assumed that ocean circulation and tides are key drivers for sea ice stability in the Southern Ocean. According to, for example, Tamsitt et al. (2017) and Liu et al. (2018), upwelling of deeper water masses can be expected along the shelf break. Tides apparently have a great influence on the stability of the sea ice. For the Weddell Sea Koentopp (2005) state that the ocean heat loss is increased in areas with elevated tidal energy, thus leading to thinner ice. Furthermore, the mechanical stress is enhanced due to tidal currents, which are most pronounced over the shelf area and along the shelf break. In the Weddell Sea the sea ice motion is accelerated above the shelf break pointing generally toward free drifting areas. Data from drifting buoys deployed during a field campaign in the Weddell Sea show the existence of a local shear zone following the shelf break leading to strong divergence and deformation processes in the sea ice cover (Heil et al., 2008; Hutchings et al., 2012). This observation can be confirmed by the model results shown in Figure 4b, where the zone of divergence (black arrow) follows the continental slope but also by Stewart et al. (2019) who verified the position of the Antarctic Slope current in detail. A local reduction of up to 15% in sea ice concentration is caused by tides, and on average a reduction by 3–10% is expected (Koentopp, 2005). Therefore, the formation of leads is favored in areas of strong tidal currents. Padman and Kottmeier (2000) describe the tidal currents in the Weddell Sea to be strong above the shelf and along the shelf break increasing the mechanical stress on the ice cover. Robertson et al. (1998) show results for modeled tidal constituents, two for semidiurnal and two for diurnal cycles. In particular, over the shelf break the diurnal major axis length increases, which indicates stress that is induced into the sea ice. Mack et al. (2013) find that an effect of tides is decreasing the sea ice concentration for an area at the shelf break in the Ross Sea. The authors analyzed subdaily AMSR-E passive microwave data and found that tides explain most of the variance in the wintertime sea ice concentration. Although the above-mentioned studies focus on smaller areas and shorter time periods, their findings support large-scale modeling studies.

Only recently, Stewart et al. (2019) highlighted the connection between the amplitude of tidal flows across the continental shelf break and sea ice in the Southern Ocean based on a detailed model study. Their work indicates the position of a jet in the time-mean flow speed (see Figure 1 in their paper) to follow almost perfectly the strong linear patterns of increased lead frequencies over the shelf break that we obtain from our observations (Figure 1). Additional consistencies between their model study and our data can be found in the proximity of significant bathymetric structures, for example, Maud Rise, Gunnerus Ridge, and Iselin Bank. Stewart et al. (2019) also show that the mean sea ice velocity is increased in the slope current, hence leading to more mechanical stress. All these factors favor sea ice divergence, thus causing a fracturing of the pack ice and the formation of leads. Also, previous model studies give rise to the assumption that areas of increased lead frequencies are connected to the location of the relatively warm Antarctic Slope Current (Hellmer et al., 2012; Kerr et al., 2018; Schmidtko et al., 2014). Our data, obtained from satellite observations, support many

of the hypothesized and modeled processes mentioned above. A direct comparison of lead frequencies in the Weddell Sea and surface ocean currents and divergence including tides confirms a systematic relation (Figure 4). Our data suggest that sea ice leads are generally ubiquitous features in Antarctic sea ice with a significant spatial variability that follows bathymetry.

5. Conclusions

This study presents the first high-resolution climatology of sea ice leads for the Southern Ocean for the winter months between 2003 and 2018. In particular, an overall distribution of leads in the Antarctic sea ice can be seen with pronounced patterns associated to the shelf break and several seabed ridges. The lead frequency can be as high as 0.4 in certain areas, for example, along the shelf break in the Weddell Sea. The position of the regions with the highest lead frequencies significantly supports model results of the influence of tidal and surface currents on sea ice stability. The long-term average lead frequency distribution of our study suggests a strong relationship between leads, bathymetry, and associated tides and currents.

Acknowledgments
The research was funded by the Deutsche Forschungsgemeinschaft (DFG) in the framework of the priority program "Antarctic Research with comparative investigations in Arctic ice areas" under Grants HE 2740/22 and WI 3314/3. All processing and data visualization is done in Python3.6, QGIS 3.8 and Quantarctica V3. U. H. was supported by the European Research Council (ERC) under the European Union's Horizon 2020 research and innovation program (Grant Agreement 637770). All data for this paper are properly cited and referred to in the reference list. The supplementary data are available at the online archive PANGAEA (https://doi.pangaea.de/10.1594/PANGAEA.906767). Thanks also to Hartmut Hellmer for personal communication and advise. We thank Jennifer Hutschings and one anonymous reviewer for their helpful comments.

References

Alam, A., & Curry, J. (1995). Lead-induced atmospheric circulations. *Journal of Geophysical Research*, *100*(C3), 4643. https://doi.org/10.1029/94jc02562

Chechin, D. G., Makhotina, I. A., Lüpkes, C., & Makshtas, A. P. (2019). Effect of wind speed and leads on clear-sky cooling over Arctic sea ice during polar night. *Journal of the Atmospheric Sciences*, *76*(8), 2481–2503. https://doi.org/10.1175/jas-d-18-0277.1

Fraser, A. D., Massom, R. A., Michael, K. J., Galton-Fenzi, B. K., & Lieser, J. L. (2012). East Antarctic landfast sea ice distribution and variability, 2000–08. *Journal of Climate*, *25*(4), 1137–1156. https://doi.org/10.1175/jcli-d-10-05032.1

Haid, V., Timmermann, R., Ebner, L., & Heinemann, G. (2015). Atmospheric forcing of coastal polynyas in the south-western Weddell Sea. *Antarctic Science*, *27*(4), 388–402. https://doi.org/10.1017/s0954102014000893

Heil, P., Hutchings, J. K., Worby, A. P., Johansson, M., Launiainen, J., Haas, C., & Hibler, W. D. (2008). Tidal forcing on sea-ice drift and deformation in the western Weddell Sea in early austral summer, 2004. *Deep Sea Research Part II: Topical Studies in Oceanography*, *55*(8-9), 943–962. https://doi.org/10.1016/j.dsr2.2007.12.026

Hellmer, H. H., Kauker, F., Timmermann, R., Determann, J., & Rae, J. (2012). Twenty-first-century warming of a large Antarctic ice-shelf cavity by a redirected coastal current. *Nature*, *485*(7397), 225–228. https://doi.org/10.1038/nature11064

Holland, P. R., & Kwok, R. (2012). Wind-driven trends in Antarctic sea-ice drift. *Nature Geoscience*, *5*(12), 872–875. https://doi.org/10.1038/ngeo1627

Hutchings, J. K., Heil, P., Steer, A., & Hibler, W. D. (2012). Subsynoptic scale spatial variability of sea ice deformation in the western Weddell Sea during early summer. *Journal of Geophysical Research*, *117*, C01002. https://doi.org/10.1029/2011jc006961

Kern, S. (2009). Wintertime Antarctic coastal polynya area: 1992–2008. *Geophysical Research Letters*, *36*, L14501. https://doi.org/10.1029/2009gl038062

Kerr, R., Dotto, T. S., Mata, M. M., & Hellmer, H. H. (2018). Three decades of deep water mass investigation in the Weddell Sea (1984–2014): Temporal variability and changes. *Deep Sea Research Part II: Topical Studies in Oceanography*, *149*, 70–83. https://doi.org/10.1016/j.dsr2.2017.12.002

Koentopp, M. (2005). Influence of tides on sea ice in the Weddell Sea: Investigations with a high-resolution dynamic-thermodynamic sea ice model. *Journal of Geophysical Research*, *110*, C02014. https://doi.org/10.1029/2004jc002405

Liu, C., Wang, Z., Cheng, C., Wu, Y., Xia, R., Li, B., & Li, X. (2018). On the modified circumpolar deep water upwelling over the Four Ladies Bank in Prydz Bay, East Antarctica. *Journal of Geophysical Research: Oceans*, *123*, 7819–7838. https://doi.org/10.1029/2018jc014026

Lüpkes, C., Vihma, T., Birnbaum, G., & Wacker, U. (2008). Influence of leads in sea ice on the temperature of the atmospheric boundary layer during polar night. *Geophysical Research Letters*, *35*, L03805. https://doi.org/10.1029/2007gl032461

Mack, S., Padman, L., & Klinck, J. (2013). Extracting tidal variability of sea ice concentration from AMSR-E passive microwave single-swath data: A case study of the Ross Sea. *Geophysical Research Letters*, *40*, 547–552. https://doi.org/10.1002/grl.50128

Madec, G. (2008). *NEMO ocean engine*. France: Note du Pôle de modélisation, Institut Pierre-Simon Laplace (IPSL). ISSN No 1288-1619.

Marcq, S., & Weiss, J. (2012). Influence of sea ice lead-width distribution on turbulent heat transfer between the ocean and the atmosphere. *The Cryosphere*, *6*(1), 143–156. https://doi.org/10.5194/tc-6-143-2012

Maykut, G. A. (1978). Energy exchange over young sea ice in the central Arctic. *Journal of Geophysical Research*, *83*(C7), 3646. https://doi.org/1029/jc083ic07p03646

Maykut, G. A. (1982). Large-scale heat exchange and ice production in the central Arctic. *Journal of Geophysical Research*, *87*(C10), 7971. https://doi.org/10.1029/jc087ic10p07971

Müller, M., Batrak, Y., Kristiansen, J., Køltzow, M. A. Ø., Noer, G., & Korosov, A. (2017). Characteristics of a convective-scale weather forecasting system for the European Arctic. *Monthly Weather Review*, *145*(12), 4771–4787. https://doi.org/10.1175/mwr-d-17-0194.1

Murashkin, D., Spreen, G., Huntemann, M., & Dierking, W. (2018). Method for detection of leads from Sentinel-1 SAR images. *Annals of Glaciology*, *59*(76pt2), 124–136. https://doi.org/10.1017/aog.2018.6

Ohshima, K. I., Fukamachi, Y., Williams, G. D., Nihashi, S., Roquet, F., Kitade, Y., et al. (2013). Antarctic Bottom Water production by intense sea-ice formation in the Cape Darnley polynya. *Nature Geoscience*, *6*(3), 235–240. https://doi.org/10.1038/ngeo1738

Padman, L., Fricker, H. A., Coleman, R., Howard, S., & Erofeeva, L. (2002). A new tide model for the Antarctic ice shelves and seas. *Annals of Glaciology*, *34*, 247–254. https://doi.org/10.3189/172756402781817752

Padman, L., & Kottmeier, C. (2000). High-frequency ice motion and divergence in the Weddell Sea. *Journal of Geophysical Research*, *105*(C2), 3379–3400. https://doi.org/10.1029/1999jc900267

Paul, S., Willmes, S., & Heinemann, G. (2015). Long-term coastal-polynya dynamics in the southern Weddell Sea from MODIS thermal-infrared imagery. *The Cryosphere*, *9*(6), 2027–2041. https://doi.org/10.5194/tc-9-2027-2015

Röhrs, J., & Kaleschke, L. (2012). An algorithm to detect sea ice leads by using AMSR-E passive microwave imagery. *The Cryosphere*, *6*(2), 343–352. https://doi.org/10.5194/tc-6-343-2012

Riggs, G. A., & Hall, D. K. (2015). MODIS Sea Ice Products User Guide to Collection 6 (Technical Report). Boulder, CO, USA: National Snow and Ice Data Center, University of Colorado.

Robertson, R. (2005). Baroclinic and barotropic tides in the Weddell Sea. *Antarctic Science*, *17*(03), 461. https://doi.org/10.1017/s0954102005002890

Robertson, R., Padman, L., & Egbert, G. D. (1998). Tides in the Weddell Sea, *Ocean, Ice, and Atmosphere: Interactions at the Antarctic Continental Margin* (pp. 341–369). Washington, DC: American Geophysical Union. https://doi.org/10.1029/ar075p0341

Schaffer, J., & Timmermann, R. (2016). Greenland and Antarctic ice sheet topography, cavity geometry, and global bathymetry (RTopo-2), links to NetCDF files. (data set). PANGAEA,https://doi.org/10.1594/PANGAEA.856844, Supplement to: Schaffer, Janin; Timmermann, Ralph; Arndt, Jan Erik; Kristensen, Steen Savstrup; Mayer, Christoph; Morlighem, Mathieu; Steinhage, Daniel (2016): A global, high-resolution data set of ice sheet topography, cavity geometry, and ocean bathymetry. Earth System Science Data, 8(2), 543-557, https://doi.org/10.5194/essd-8-543-2016, .

Schmidtko, S., Heywood, K. J., Thompson, A. F., & Aoki, S. (2014). Multidecadal warming of Antarctic waters. *Science*, *346*(6214), 1227–1231. https://doi.org/10.1126/science.1256117

Smith, S. D., Muench, R. D., & Pease, C. H. (1990). Polynyas and leads: An overview of physical processes and environment. *Journal of Geophysical Research*, *95*(C6), 9461. https://doi.org/10.1029/jc095ic06p09461

Spreen, G., Kaleschke, L., & Heygster, G. (2008). Sea ice remote sensing using AMSR-E 89-GHz channels. *Journal of Geophysical Research*, *113*, C02S03. https://doi.org/10.1029/2005jc003384

Stewart, A. L., Klocker, A., & Menemenlis, D. (2019). Acceleration and overturning of the Antarctic Slope Current by winds, eddies, and tides. *Journal of Physical Oceanography*, *49*, 2043–2074. https://doi.org/10.1175/jpo-d-18-0221.1

Stirling, I. (1997). The importance of polynyas, ice edges, and leads to marine mammals and birds. *Journal of Marine Systems*, *10*(1), 9–21. https://doi.org/10.1016/S0924-7963(96)00054-1

Tamsitt, V., Drake, H. F., Morrison, A. K., Talley, L. D., Dufour, C. O., Gray, A. R., et al. (2017). Spiraling pathways of global deep waters to the surface of the Southern Ocean. *Nature Communications*, *8*(1). https://doi.org/10.1038/s41467-017-00197-0

Tamura, T., Ohshima, K. I., & Nihashi, S. (2008). Mapping of sea ice production for Antarctic coastal polynyas. *Geophysical Research Letters*, *35*, L07606. https://doi.org/10.1029/2007gl032903

Turner, J., Hosking, J. S., Bracegirdle, T. J., Marshall, G. J., & Phillips, T. (2015). Recent changes in Antarctic Sea Ice. *Philosophical Transactions of the Royal Society A: Mathematical, Physical and Engineering Sciences*, *373*(2045), 20140163. https://doi.org/10.1098/rsta.2014.0163

Wang, Q., Danilov, S., Jung, T., Kaleschke, L., & Wernecke, A. (2016). Sea ice leads in the Arctic Ocean: Model assessment, interannual variability and trends. *Geophysical Research Letters*, *43*, 7019–7027. https://doi.org/10.1002/2016gl068696

Willmes, S., & Heinemann, G. (2015). Pan-Arctic lead detection from MODIS thermal infrared imagery. *Annals of Glaciology*, *56*(69), 29–37. https://doi.org/10.3189/2015aog69a615

Willmes, S., & Heinemann, G. (2016). Sea-ice wintertime lead frequencies and regional characteristics in the Arctic, 2003–2015. *Remote Sensing*, *8*(1), 4. https://doi.org/10.3390/rs8010004

Zwally, H. J., Comiso, J. C., & Gordon, A. L. (1985). Antarctic offshore leads and polynyas and oceanographic effects, *Oceanology of the antarctic continental shelf* (pp. 203–226). Washington, D.C.: American Geophysical Union. https://doi.org/10.1029/ar043p0203